

The problem of laser-pulse non-ideality in non-linear laser-based diagnostics

M. Marrocco

ENEA – Casaccia – Via Anguillarese 301, 00060 S. M. di Galeria (Rome), Italy

Abstract

Non-ideality of laser pulses is due to uneven spatial, temporal and spectral distributions of laser beams. Unfortunately, such deviations from hypothetical regular laser profiles are crucial for the correct data interpretation of measurements obtained in some diagnostic applications of non-linear spectroscopy. In this Lecture, methods to circumvent wrong interpretation of spectroscopic data will be presented. To that end, the problem will be specified to incoherent non-linearity that is typical for saturated behavior in fluorescence spectroscopy. Traditional solutions will be briefly recalled and new methods will be discussed.

Introduction

In laser spectroscopy, any reliable quantitative elaboration of spectroscopic data must include the influence of the realistic experimental conditions [1, 2]. In particular, spectroscopic techniques, prone to non-linear features, might experience a non-negligible sensitivity to the so-called laser-wing contribution [2]. This unwanted effect arises from the threefold non-ideality of laser beams in the spatial, temporal and spectral domains. The non-ideality is understood in terms of laser-intensity distributions which are far from being regular like in the ideal case of Fig. 1.

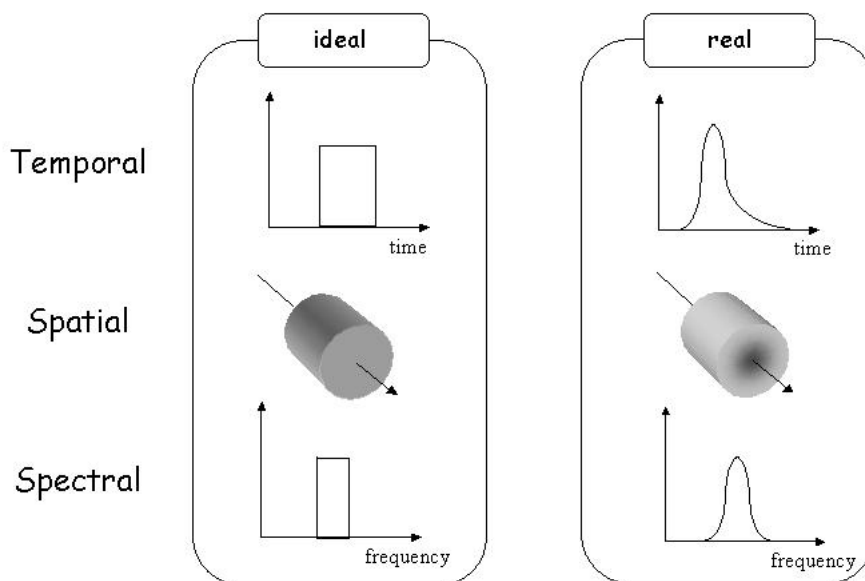


Fig. 1. Laser intensity distributions in temporal, spatial and spectral domains for ideal and realistic conditions.

Although ideal approaches provide a good theoretical framework to simplify the understanding of spectroscopic experiments, more realistic uneven distributions are instead expected and a correct procedure to account for their contribution must be assumed. The problem can be exactly defined with the help of Fig. 2. Let us call $I(\mathbf{r}, t, \nu)$ the distribution of laser intensity depending on spatial position $\mathbf{r} = (x, y, z)$, time t and frequency ν . If $I(\mathbf{r}, t, \nu)$ is the input of our system, then the interaction between laser and matter can be represented by an operator \hat{O} determined by the result M of our measurement, such that $M = \hat{O} I(\mathbf{r}, t, \nu)$.

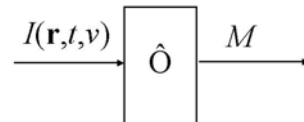


Fig. 2. The spectroscopic outcome M of a measurement can be thought as the result of an operator \hat{O} applied to the input laser profile $I(\mathbf{r}, t, \nu)$.

In linear spectroscopy, the result M is proportional to the total laser irradiance $I_{0\nu}$, that is $M = k I_{0\nu}$, and laser wing contribution is completely uninfluential. On the contrary, the problem becomes critical when linearity does not hold anymore ($M \neq k I_{0\nu}$) and, in principle, laser wing contribution cannot be worked out, unless the physics of interaction has been exactly described. Usually, in molecular physics, one cannot be sure how laser peaks add to the signal with respect to the associated laser wings and then realistic distributions of laser beams must somehow be taken into account. However, a distinction is necessary: incoherent spectroscopies are more sensitive to laser-wing effects than coherent spectroscopies. This is the direct consequence of two main facts. First, the incoherent scattering over the whole solid angle disperses the information on spatial dependence (this is not so in coherent spectroscopy where directional properties of laser beams are kept). Second, time responses of incoherent signals are generally altered if compared to the exciting laser pulses (whereas coherent signals follow quite well the time evolution of laser pulses). For these reasons, the discussion considered in this paper will be limited to more problematic spectroscopies as those based on fluorescence. In particular we will consider saturation behavior in Laser Induced Fluorescence (LIF) [1, 2] and Fluorescence Correlation Spectroscopy (FCS) [2, 3]. Recent results obtained by the author will be reported and some short considerations about a coherent application of fluorescence, namely super-radiance in Photon-Echo Spectroscopy [1], will also be presented.

Laser-wing effects in Saturated LIF

Saturated laser-induced fluorescence (SatLIF) is an important spectroscopic technique that has attracted a great deal of attention because of its diagnostic potential for species detection in combustion science [1, 2]. However, one of its major limitations stems from the realistic characteristics of laser pulses; spectral, spatial and temporal laser-wings are in fact unavoidably generated with laser action and this implies that saturation efficiencies in the optical response from the excited medium are determined by a compromise between contributions of laser peaks and their corresponding wings [2]. But the success of a SatLIF experiment relies on the achievement of the

highest saturation status and experimental data become useless if wing contributions have not been cautiously eliminated [2]. Therefore it is necessary to find out suitable methods which are capable of efficient data reduction so as to minimize laser-wing influences on data quality.

Spectral wings are generally easy to ponder because spectral distributions of both the laser and the interacting medium are quite known with a good level of approximation. Nonetheless, it must be said that the effect of spectral distributions is moderate because it is seen in the increase of total laser irradiance to counterbalance the spread over the relevant range of frequencies belonging to laser line and molecular absorption band. In symbols, $I_{0v} \rightarrow \Gamma I_{0v}$ where Γ is the spectral overlap integral between the laser and the absorption line [4]. Therefore, spectral laser wings do not entail a substantial alteration in the understanding of the spectroscopic signal except for an increase of a factor $1/\Gamma$ in realistic laser irradiances. More critical is the influence of spatial and temporal wings for which the relevant laser parameter is the laser intensity $I(\mathbf{r}, t, \nu)$. If F is the local fluorescence, then the result of a measurement is the spatio-temporal integral Φ

$$\Phi(t, I_{0v}) = \int F[t, I(\mathbf{r}, t, \nu)] d\mathbf{r} dt, \quad (1)$$

and it is understood that the functional forms of F and Φ cannot be the same when F is non-linear. Suppose, for instance, to saturate a molecular transitions as in Fig. 3 where the continuous line reproduces an ideal behavior of F . For a given laser irradiance (or laser intensity), the ideal experimental conditions are those represented by the point A. Spectral wings shift the realistic point from A to B according to the value of the overlap integral Γ . But, in addition to the horizontal translation along the curve, the integral in Eq. (1) introduces a drastic change in the fluorescence dependence on spectral irradiance I_{0v} . This means that the location of realistic conditions is more properly determined by a point C that is far from the ideal behavior given by the continuous line.

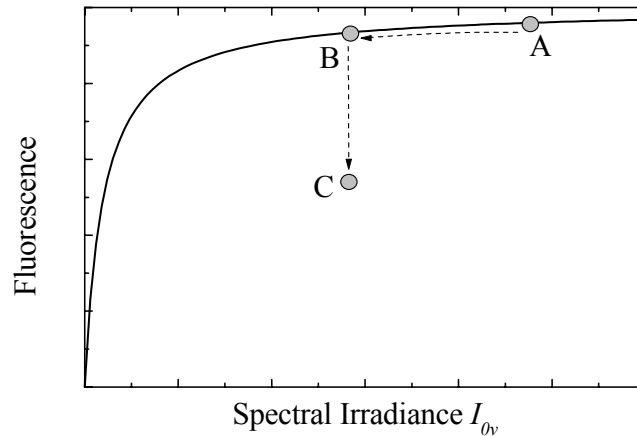


Fig. 3. Fluorescence versus total spectral irradiance. The line reproduces the ideal saturated behavior. The effect of spectral laser wings is given in the shift of the ideal experimental conditions from the point A to point B. Spatial and temporal laser wing contributions determine the location of point C.

From these preliminary considerations, it is clear that spectral influences of laser wings are not so poignant as temporal and spatial alterations. This is the reason why we will deal with such latter contributions only. Traditional and new methods to treat spatial and temporal wings will be elucidated for SatLIF and the discussion will be extended to Fluorescence Correlation Spectroscopy (FCS) later on.

Traditional approaches to temporal and spatial wings in SatLIF

Temporal wing effects have been theorised in simple dynamical models [5, 6] and measured as well [5]. Since then, time sampling of fluorescence has customarily been used [7]. In this manner, the laser-peak contribution is retained whereas the remaining ambiguous portions of the signal are discarded.

In time resolved measurements, the signal $S(t)$ of Fig. 4 is sampled around its maximum value S_{\max} with a gate width t_g that is rather short. Typically, t_g is significantly shorter than the time width t_L of the laser pulse. In this way good laser-wing suppression is ensured and a stationary signal can be assumed within the chosen gate. The result of signal sampling is then

$$E_g = \int_{t_0}^{t_0+t_g} S(t)dt = S_{\max} \cdot t_g \quad (2)$$

where E_g is the energy collected within the gate and t_0 is the gate starting time which is supposed to be close to the arrival time of S_{\max} .

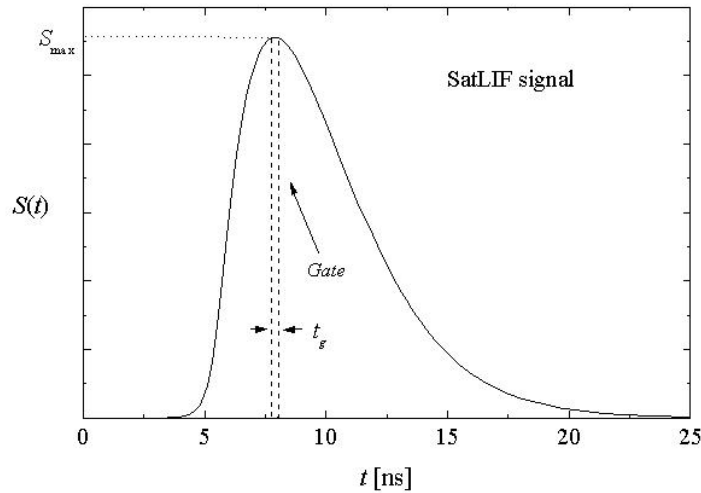


Fig. 4. SatLIF signal and its time sampling

The saturation status is usually evaluated by measuring E_g as a function of the spectral laser irradiance I_{0v} (or related variables) [2] and this is enough to avoid wing effects that add up in the integration of the whole signal. Eq. (2) suggests, moreover, that if S_{\max} is possibly measured with an oscilloscope it is not necessary to carry out time sampling. On the other hand, considerations about noise, acquisition rate and data elaboration dissuade experimentalists from taking S_{\max} with oscilloscopes. Therefore this kind of measurement will be disregarded. An additional problem in Eq. (2) arises from the retardation of S_{\max} . The time t_0 corresponding to the signal maximum changes with the laser irradiance [8]. Thus an opportune choice of t_0 for each value of I_{0v} must be considered to determine properly the saturation curve $E_g(I_{0v})$.

So much for the ordinary correction of temporal wings. The other relevant component of the problem is the influence of spatial wings induced by the spatial distribution of energy within laser beams. Unlike temporal corrections, a unique procedure does not exist and therefore we list here the different approaches developed in the past decades. Rodrigo and Measures recognized the effect

in a plasma [9]. Later, fictitious saturated volumes were proposed to subtract laser-wings during data reduction [10]. This approach was introduced in experiments [11] and critics to the accuracy of number densities, calculated under the hypothesis of uniform laser profiles, were outlined [12]. The occurrence of spatial effects with gaussian laser beams was also studied [13]. Since then, some authors have employed the simplest solution of spatial selection operated by collection optics aligned with a monochromator slit carefully adjusted to image spatial peaks of fluorescence [7], while others have designed a more complex geometry with two detection equipments (TOPLIF method) [14]. Backscattering has been suggested as well [2].

In each of the previous proposals spatial determination of maximal emission within the interaction volume is ensured and spatial laser-wings are minimized. Note, however, that their contribution is not totally eliminated because of the approximations introduced. For instance, spatial wings still contribute along the direction of observation with one monochromator slit, no matter how good the spatial selection is for the other relevant directions. Realizations with two orthogonal detection equipments might overcome this problem, but, besides the experimental difficulties, theory is limited to steady-state of a two-level molecular system [14]. In conclusion, unwanted contributions from laser-wings for realistic experiments might be reduced to a good level of negligibility but large signal losses, finite spatial resolution and experimental efforts (especially in the TOPLIF method where two complete and well aligned detection systems are simultaneously employed) are unavoidable.

Salmon and Laurendeau have suggested the idea of searching for fluorescence emitted from the line traced by the spatial maximum (center-line) of laser beams with gaussian or similar profiles [15]. They demonstrated that all the wing-related failures in SatLIF data are absent when the geometrical source of fluorescence is reduced to the center-line. To that end, they developed a formalism where center-line emission was derived from lateral fluorescence intensities through an Abel-like inversion [16]. Nonetheless the analysis suffers of many drawbacks that have been outlined by the author of this Lecture [17].

All in all, it should be noticed that the combined procedures for space and time corrections have the benefit of limiting the problems with laser wings but they bear the disadvantage of wasting useful portions of the signal joined with the compulsory requirement of sophisticated electronics, which are essential to gate the fast optical response of the medium. The disadvantages could be very critical in those cases where either a weak signal is expected or a fast sampler is unavailable. Therefore methods offering alternative approaches are welcome if they save in the signal what the selective procedures for space and time corrections throw away.

New methods for laser-wing corrections in SatLIF

Innovative developments in wing corrections have been recently published [17, 18, 19]. In this paragraph, the key ideas which are at the basis of these new methods will be summarized. But the reader should refer to the published works for more detailed information.

Temporal corrections. It has been shown in the previous paragraph that time-sampling approach is quite harsh but is so intuitively simple that experimentalists have not been stimulated to try other alternatives which might be useful to circumvent the troubles of the time resolved technique (TRT). As a consequence, the TRT has been silently accepted as an ordinary tool of a well planned SatLIF experiment. However, numerical simulations with quasi-realistic laser pulses have suggested the possibility of temporal laser-wing corrections based on fluorescence power [18]. In that proposal, the wing contribution in the fluorescence energy is counterbalanced by the same wing contribution in the temporal extension of fluorescence. The ratio between energy and time width should be wing-free and good numerical results have been found with quasi-symmetric time signals obtained from simple molecular models.

The general idea of this novel procedure can be described as follows. First of all, consider the acquisition of the entire pulse $S(t)$ of Fig. 2. The result is the energy content E of the whole pulse

$$E = \int_0^{\infty} S(t) dt . \quad (3)$$

Note that in Eq. 3 wing contribution is not disregarded. But, this contribution does not affect the energy E only, but the time width t_F of $S(t)$ as well. If we are able to transfer in t_F the same wing contribution contained in E , the ratio E / t_F will be error free. The definition of t_F is then the core of our thesis and it deserves a correct assessment.

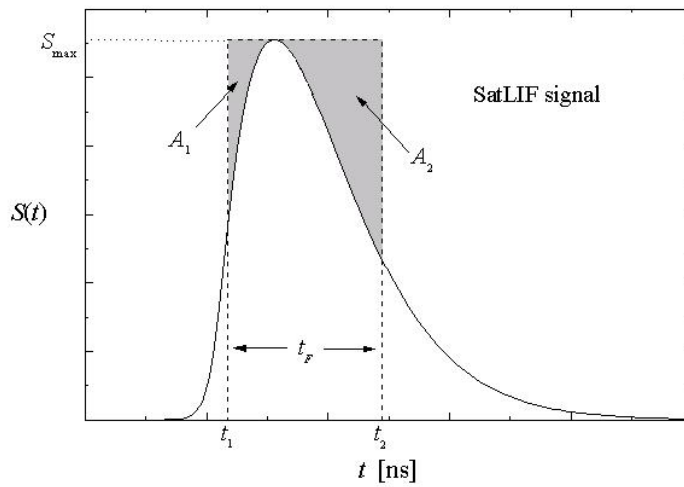


Fig. 5. Same signal of Fig. 4 with the fictitious gate used for power measurements.

Fig. 5 shows the same signal $S(t)$ of Fig. 4. Suppose to insert in the figure a fictitious rectangular area similar to the gate of Fig. 4, with the same amplitude S_{\max} but with a larger width. Its starting time t_1 is chosen such that the filled area A_1 in the rectangle equals the initial portion of the signal area that is out of the rectangle,

$$A_1 = \int_0^{t_1} S(t) dt . \quad (4)$$

In the same fashion, we define the imaginary gate end t_2 so that

$$A_2 = \int_{t_2}^{\infty} S(t) dt \quad (5)$$

and the time t_F remains determined by the difference between t_2 and t_1 . This definition of t_F leads to the equality between the pulse energy E in Eq. (3) and the total rectangular area A . If a power measurement with t_F is thus performed, its result is

$$P = \frac{E}{t_F} = \frac{A}{t_F} = S_{\max} \quad (6)$$

and Eq. (6) is now free from wing contribution! This means that, according to Eqs. (3)-(6), a power measurement yields the maximum of the signal, without the additional assumption of a steady signal within the gate as was needed for time resolved measurements. But there is another conclusion that follows from the comparison of Eq. (6) with Eq. (2). In the proposed method, the saturation status evaluated from the curve $P(I_{0v})$ is independent from any time delay of $S(t)$ or S_{\max} . Fine synchronization (needed in TRT to adjust t_0) does not matter at all. In addition, complete saturation (or steady state) can be detected even if it lasts for intervals shorter than the time gate t_g employed in TRT.

The application of Eq. (6) is founded on the experimental determination of the total energy E and the characteristic time t_F . The energy E is given by the integration of the whole pulse measured with a photodetector. This is particularly relevant to work out species concentrations. In fact, considerations about signal-to-noise ratio (S/N) makes E a better quantity to elaborate than E_g obtained with TRT measurements. The improvement in S/N goes with $(t_F / t_g)^{1/2}$ and it is about one order of magnitude when t_F , associated to good levels of saturation, is compared with typical values of t_g .

The measure of t_F is, however, quite subtle. Apparently, the characteristic fluorescence time t_F can be obtained easily with an oscilloscope. Once again, an acquisition of $S(t)$ with an oscilloscope would give a direct measure of S_{\max} without resorting to any gate or power measurement whatsoever. But requirements about sampling speed, data interpretation and S/N do not support such a hasty method. What is more, fluorescence is the radiative emission specified by $N_{ex}Ah\nu$, with N_{ex} the excited molecular population, A the spontaneous emission rate and $h\nu$ the photon energy. This means that the generic term “fluorescence” has a physical translation in terms of power. Hence measuring fluorescence implies a reference to finite time intervals. In the present case, the determination of t_1 and t_2 can be very precise if interpolation is applied to data points taken from $S(t)$ with an ordinary oscilloscope. Interpolating routines can characterize the rise and fall of SatLIF signals very well, even if oscilloscope sampling is not so fast compared to the laser pulse. An example will be provided shortly. But, the additional aspect to be considered is the detector time response, that introduces an undesirable distortion in the real signal profile $S(t)$. The distortion depends on the detector response function and its removal is recommended for a more precise data analysis. This problem is nowadays limited by the availability of fast detectors. Their rise time is typically well below 1 ns and their contribution to the signal can be deconvolved from measured data. The correction for the detector response is of course more necessary for very short laser pulses, but it becomes less important with longer and energetic laser pulses that guarantee time widths of several tens of ns in the fluorescence response. To simplify our problem we suppose to have well characterized our detector so that its contribution has been sorted out.

To exemplify how the proposed method works, a simple dynamical scheme of a four-level molecule was considered. Simulations were run with SatLIF signals obtained as wide-band transient solutions of rate equations associated with the simplified molecule irradiated with a Q-switched laser pulse of temporal length $t_L = 5$ ns. Analytical solutions were impossible and we resorted to numerical methods. The parameters were deduced for a transition in the $A^2\Sigma^+(v'=0)-X^2\Pi(v''=0)$ band of hydroxyl radical. Rotational manifolds in the band were lumped together to form the two levels not coupled by the laser. A sampling at $r_s = 1$ GS/s (i.e. one point each ns) of $S(t)$ was assumed to simulate data acquisition at the oscilloscope. This is in agreement with not advanced sampling rates available on the market. Fig. 6 reports the relative deviation $\eta = 100(1 - P/S_{\max})$ normalized to S_{\max} . The TRT uncertainty (open circles) has an oscillation caused by the changing phase delay in $S(t)$. A run with a variable t_0 , linked to the signal maximum, made the oscillation disappear. Note now the result for FTP measurements (solid circles). The uncertainty η is within 2 % at irradiances that are not so relevant for the highest saturation. The chaotic behaviour is of course due to the combined effect between the finite sampling rate r_s and the randomness of the

oscilloscope clock. But, regardless of the oscilloscope performances, η is better regularised at higher laser irradiances, where the saturation prediction is practically without flaws.

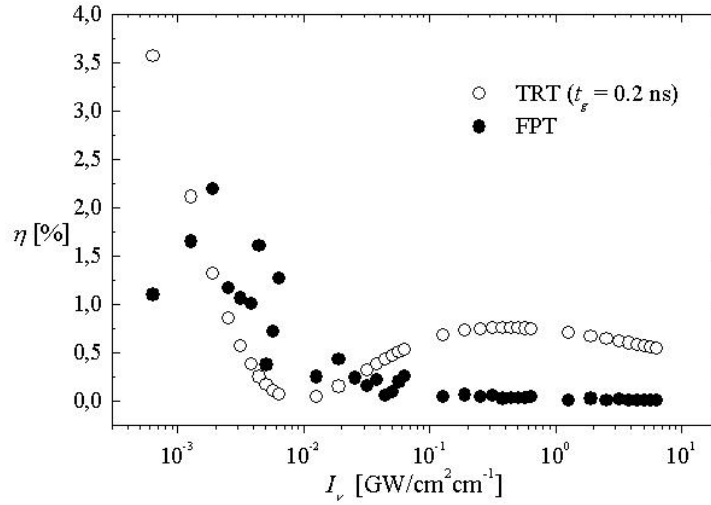


Fig. 6. Comparison between time sampling (TRT) and power measurements (FPT) in terms of uncertainty η .

The sensitivity to changes in the physical model was checked and the new method of FPT performed well. It is worth saying that FPT corrections of laser wings were significantly better than TRT corrections when fluctuations in laser pulse had been included.

Spatial corrections. The other relevant source of error is the spatial component of laser-wing contribution. In this context, data corrections will be based on the original idea of Salmon and Laurendeau of center-line detection [15]. Their Abel-like data reduction will be avoided with a different procedure that will be outlined hereafter [17].

Experiments with induced saturation [1, 7] are carried with focused gaussian laser beams and Eq. (1) contains a surface integral

$$\Phi(t, I_0) = k l \int F(t, I(x, y, t)) dx dy, \quad (7)$$

where l is the length of the interaction volume along the laser propagation direction (i.e. z-axis). We notice now that gaussian laser beams can be separated in their radial, angular and temporal component

$$I(\rho, \vartheta, t) = I_0 R(\rho) \Theta(\vartheta) T(t) = I_{rad}(\rho) \Theta(\vartheta) T(t). \quad (8)$$

This is very advantageous because, after simple manipulation, it is possible to obtain the following inversion formula [17]

$$F(t, I(\rho = 0, t)) = \frac{2}{k \pi w^2 l} I_0 \frac{d\Phi(t, I_0)}{dI_0} \quad (9)$$

where the fluorescence signal F is the center-line emission defined by $\rho = 0$. This means that laser-wing contribution can be totally sorted out by measuring the fluorescence signal Φ relative to the whole interaction region!

A simulation with the four-level molecule used in Fig. 6 with relevant quenching and rotational relaxation was run. We just recall that molecular parameters were derived for the emission of the $A^2\Sigma^+(v'=0)-X^2\Pi(v''=0)$ band in hydroxyl radical at atmospheric pressure. Time profiles of $F(t, I(\rho=0, t))$ and $\Phi(t, I_0)$ have been reported in Fig. 7.

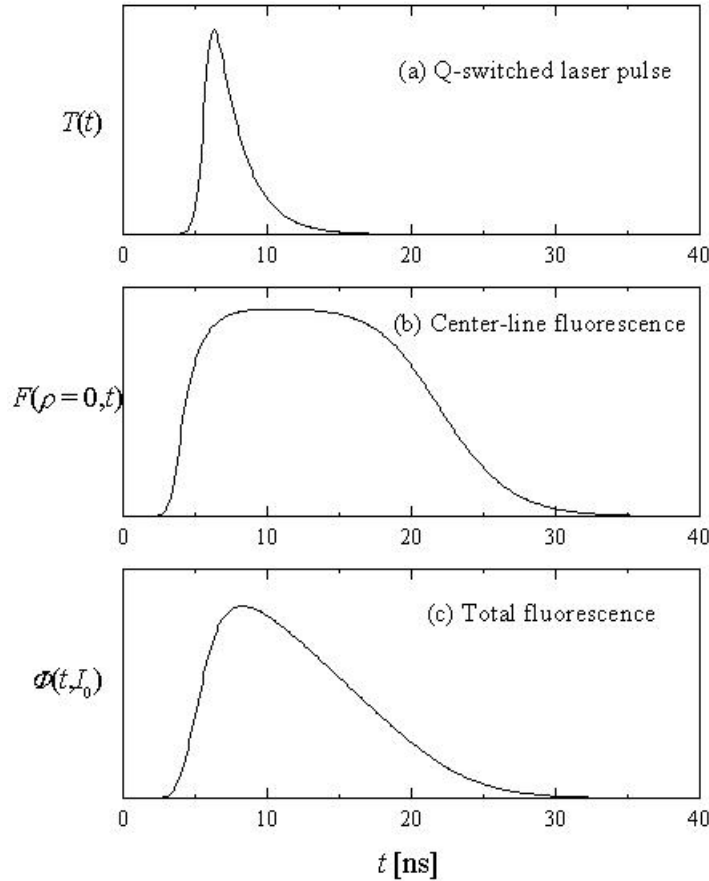


Fig. 7. Time profiles of (a) Q-switched laser pulse T , (b) center-line fluorescence F and (c) total fluorescence Φ .

High saturation can be observed in Fig. 7(b). Actually, saturation reaches completeness in the remarkable plateau that lasts for some ns. On the contrary, Fig. 7(c) shows the loss of saturation quality that is observable with acquisitions of the signal Φ . The plateau has disappeared and the time structure is similar to the laser pulse but with a more enlarged time width determined by the complex interplay between molecular dynamics and time shape of the laser pulse. Unfortunately the sole longer width of the signal is not sufficient to detect the high saturation status established along center-line emission of Fig. 7(b).

To overcome this problem, experimentalists have tried to select a region around the spatial maximum of the laser profile. For instance, a combination of lenses and a monochromator slit has often been employed to discriminate peaks in emitted profiles [7]. It is then interesting to compare the method here proposed to acquisitions performed in that fashion. To that end, the signal of Fig. 7(c) was again considered while the resolving slit was supposed to receive light from a region ten times smaller than the corresponding volume associated to the laser beam waist. Better resolutions are not found in literature and therefore we will limit our demand on spatial selection. The resolved total signal Φ^* is shown in Fig. 8(a) and has a shape that is rather similar to Φ (Fig. 7(c)). It is clear

that laser-wings are still significant although a consistent spatial discrimination was included. This means, in turn, that a simple spatial selection is not sufficient to correct for laser wings.

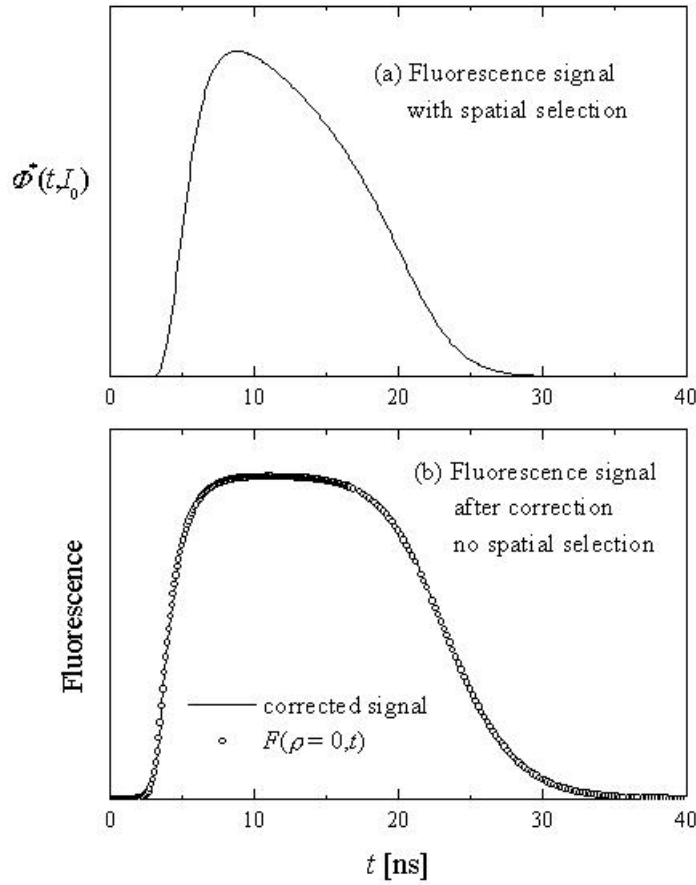


Fig. 8. Comparison between time profiles of Φ^* and F . The signal obtained with the procedure of Eq. (9) is given by the continuous line in (b)

According to Eq. (9), the derivation of Φ yields a much better result. In the simulation the derivative of Fig. 7(c) with respect to I_0 was calculated and the right-hand of Eq. (8) has been reported in the continuous line of Fig. 8(b). To compare this result with the exact center-line emission, some points (open circles) of the numerical solution of Fig. 7(b) have been included in Fig. 8(b). The two results coincide and this proves graphically and numerically what has been obtained analytically in Eq. (9).

In conclusion new methods to derive wing-free fluorescence signals have been demonstrated without using temporal and spatial selections. The generality of the new methods is such that it could be applied to any experimental condition where temporal and spatial laser profiles have been well characterized. The new methods represent a great advance in comparison to the specificities of previous proposals found in literature.

As a final remark it must be said that these techniques do not alter significantly the ordinary procedures to extract physical parameters from experimental data, but for a more qualified discussion on this issue the reader should consult the appropriate literature [1].

Extension to other techniques: Fluorescence Correlation Spectroscopy

The strategy utilized in the treatment of laser-wings in SatLIF can be applied to other spectroscopic investigations where saturation and its non-linearity play a fundamental role. This is the case of Fluorescence Correlation Spectroscopy (FCS) that is common to many scientific disciplines [1, 3]. The versatility of FCS methods stems from the fact that fluorescence and its fluctuations can be easily induced and detected under a wide range of experimental conditions. But sensitivity to changes of molecular parameters and interactions is not the sole advantage of FCS. The technique is also powerful inasmuch as the problem of single-molecule detection in gases, liquids and condense matter can be successfully tackled. Several authors have indeed reported that microscopy with proper laser characterization can be combined to give impulse to many studies and applications where single molecule detection has a key role [1, 3]. Given the context of the present meeting, for which velocimetric measurements are particularly relevant, it is also worth mentioning that studies of micro-fluid dynamics are accessible by FCS [20].

Within FCS methods aimed at single-molecule detection, fluorescence-intensity autocorrelation due to two photon excitation has received a much greater attention [3, 21]. Although fluorescence is traditionally thought as an optical response after the absorption of one photon, two-photon FCS (TPFCS) has proven to be valuable to enhance spatial resolution and background suppression in comparison with fluorescence due to one photon excitation [21]. This results from two main facts: (1) spatial resolution is determined by the superposition of two gaussian beams (supergaussian confinement), (2) noisy background is suppressed by the large difference between exciting and detected wavelength.

Among the phenomena capable of important deviations from the standard TPFCS theory there is saturation. Actually, the role played by saturation seems to be overlooked in literature where people have their struggle to understand the competition of saturation with other molecular effects like photo-bleaching and inter-system crossing (ISC) [3, 21]. The problem is of course complicated by the spatial contribution of laser-wing effects and the proposed method of spatial-wing correction [17] might be helpful to clarify the problem.

The standard theory of TPFCS

The conceptual basis of TPFCS is very simple and can be resumed from different references [3, 21]. In this paper it will be recalled briefly to have an immediate idea on how theory and fundamental equations are modified by the proposed theory.

Consider then a laser of intensity I_0 which excites a group of sparse molecules of average concentration $\langle C \rangle$. The corresponding average fluorescence signal $\langle F \rangle$ is expressed as

$$\langle F \rangle = k \langle C \rangle I_0^2 \int S(\mathbf{r}) d\mathbf{r} \quad (10)$$

where k is a constant accounting for absorption cross-section, quantum yield, collection and detection efficiencies. The spatial integral is over the three-dimensional space determined by the sample volume from which fluorescence is measured. The function $S(\mathbf{r})$ is the so-called point-spread function (PSF) which describes the spatial distribution of fluorescence.

Fluorescence fluctuations $\delta F(t)$ are determined by variations $\delta C(\mathbf{r}, t)$ of concentration according to

$$\delta F(t) = F(t) - \langle F \rangle = k I_0^2 \int \delta C(\mathbf{r}, t) S(\mathbf{r}) d\mathbf{r} \quad (11)$$

and the autocorrelation function $G(\tau)$, given by the expression

$$G(\tau) = \frac{\langle \delta F(t+\tau) \delta F(t) \rangle}{\langle F(t) \rangle^2}, \quad (12)$$

measures the time characteristics of fluorescence fluctuations.

All of the previous equations can be carry through once the spatial profile of laser intensity $I(\mathbf{r}) = I(r, z)$ has been given. The choice of a Gaussian-Lorentzian (GL) beam is by far the most important because reproduces the actual shape of the laser beams employed in such discipline [3, 21]. Then

$$I(r, z) = I_0 \frac{\exp[-2r^2 / w^2(z)]}{1 + (z / z_0)^2} \quad (13)$$

where $w^2(z) = w_0^2 [1 + (z / z_0)^2]$. In this case the PSF is given by

$$S_{GL}(r, z) = \frac{\exp[-4r^2 / w^2(z)]}{[1 + (z / z_0)^2]^2} \quad (14)$$

From Eq. (14) it is now possible to calculate the average rate of fluorescence

$$\langle F \rangle = \frac{\pi^2}{4} k w_0^2 z_0 \langle C \rangle I_0^2 \quad (15)$$

Beside the fluorescence rate $\langle F \rangle$, the other relevant quantity to characterize fluorescence fluctuations is the autocorrelation function G given in Eq. (12). Unfortunately, G cannot be calculated for GL laser beams and we resort to the approximation of the three-dimensional Gaussian (3DG) model [22], that is

$$I(r, z) = I_0 \exp[-2(r^2 / w_0^2 + z^2 / z_1^2)] \quad (16)$$

where z_1 is different from z_0 to match better Eq. (14) with

$$S_{3DG}(r, z) = \exp[-4(r^2 / w_0^2 + z^2 / z_1^2)]. \quad (17)$$

The approximation holds because the exactness of z profile is not critical in G [22]. As will soon be shown, the dependence of G on z_1 is pretty weak and thus the approximation does not compromise the final description of correlation decay. With the 3DG assumption, fluorescence rate and correlation function for diffusional problems can be easily calculated and they are

$$\langle F \rangle = \frac{\pi^{3/2}}{8} k w_0^2 z_1 \langle C \rangle I_0^2 \quad (18)$$

$$G_D(\tau) = G_D(0) \frac{1}{1 + \tau / \tau_D} \frac{1}{[1 + (w_0 / z_1)^2 \tau / \tau_D]^{1/2}} \quad (19)$$

where the characteristic decay time τ_D is related to the diffusion coefficient D according to $\tau_D = w_0^2 / (8D)$ and the amplitude $G_D(0) = 2^{3/2} / (\pi^{3/2} w_0^2 z_1 \langle C \rangle)$. In the case of mono-disperse molecules and for purely Brownian diffusion, the amplitude is inversely proportional to the number N of molecules within the sample volume, that is $G_D(0) = \gamma / N$ with $\gamma = 2^{-3/2} \cong 0.35$. Unfortunately, the diffusion process is not the sole physical phenomenon that is relevant in this matter. In standard theory, bleaching is one of the processes largely considered [21] and it has been found that a proper expression for the correlation function is obtained with a multiplicative factor

$$G_B(\tau) = G_D(\tau)[1 - B + B \exp(-k_B \tau)] / (1 - B) \quad (20)$$

where B is the bleaching fraction and k_B is photobleaching rate [23]. The contribution of triplet ISC could also be included but will be neglected as ISC is not observed in TPFCS [21].

Critics to standard theory of TPFCS

Very recently, critics to the achievements of standard interpretation of TPFCS data have been published [24]. The authors have found that fluorescence rates, zero-time amplitudes and decays of correlation functions drastically deviate from expected behaviors. They have interpreted these effects as a competition between saturation and photo-bleaching based on a model where saturation is simulated by a difference between two spatial super-gaussians describing laser excitation.

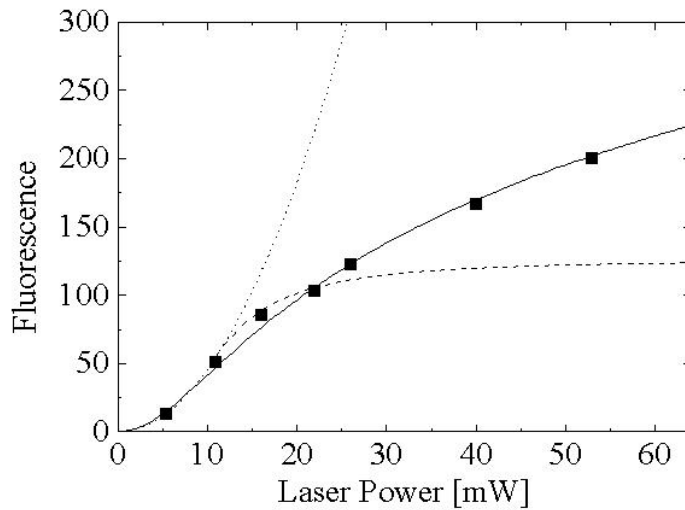


Fig. 9. Fluorescence versus laser power. The experimental points are from Ref. [24]. The dotted line is the standard square-law dependence expected for TPFCS. Dashed line represents the prediction of the model developed in Ref. [24]. The continuous line is the result of the model suggested by the author in the present text (see Eq. (22)).

An example of such deviations for fluorescence rates is given in Fig. 9, where experimental points are shown to follow the quadratic dependence (dotted line) at small laser powers only. At high laser powers, a substantial deviation is observed and the authors in Ref. [24] are able to explain it for a modest range of laser powers (dashed line). The failure of their model has been attributed to the weak adherence to the measured interaction volumes described by the actual PSF.

The troubles experienced in Ref. [24] can be recovered with a proper extension of Eq. (9). The result is already shown in Fig. 9 (continuous line) and will be explained in the following section.

Corrections to standard TPFCS theory

The main drawback of standard TPFCS theory is given by the constant reference to Eq. (19) even if the actual observation volume is altered by saturation effect. To account for this inconvenience, Eq. (9) was rearranged for the purpose of facilitating its applicability to the present case of TPFCS

$$\int S[I(r=0, z)] dz = -\frac{I_0}{\pi k} \frac{d\Sigma(I_0)}{dI_0} \quad (21)$$

where S is the local signal depending on the laser intensity profile $I(r, z) = I_0 \exp[-2r^2 / w_0^2]$ with $r = (x, y)$ defining the position in the plane perpendicular to the laser propagation axis z . The total signal Σ depends on the laser intensity I_0 and is given by the three-dimensional integration of S .

If the saturation effects are considered, then it is possible to demonstrate that the simplest expression of Σ is

$$\Sigma(I_0) = \eta I_{th}^2 \log\left(1 + \frac{I_0^2}{I_{th}^2}\right) \quad (22)$$

which is plotted in Fig. 9. The parameter I_{th} is the laser intensity that marks the threshold under which saturation effects start to become negligible.

In Fig. 9, Eq. (22) seems to match better the experimental data and thus we are encouraged to proceed further in the calculation of the autocorrelation function given in Eq. (12). Details of the calculation will be explained in a future paper, here it will be sufficient to say that the new PSF, as derived from the 3DG model when Eq. (21) is applied, is

$$S_{3DG}(r, z) = \frac{\exp[-4(r^2 / w_0^2 + z^2 / z_1^2)]}{1 + \frac{I_0^2}{I_{th}^2} \exp(-4r^2 / w_0^2)} \quad (23)$$

which reduces to Eq. (17) when $I_0 \ll I_{th}$. The new PSF enables the evaluation of the autocorrelation as well as predictions of effects due to the alteration of the probe volume. Examples are given in Fig. 10 and 11 where the amplitude and decays of the diffusional autorrelation function are reported.

In Fig. 10, the dependence of the autorrelation amplitude $G(0)$ on the laser power is shown. It tends to decrease because the observation volume increases with the laser power. In simple words, more molecules found in the laser wings contribute to the signal when laser power is increased and consequently the observation volume is enlarged. Since $G(0)$ is inversely proportional to the observation volume, the resultant effect is a decrease of $G(0)$ as Fig. 10 describes.

In Fig. 11 the time behavior of the diffusional correlation function $G(\tau)$ is given at different values of the ratio I_0 / I_{th} . The effect of volume alterations on the shape of $G(\tau)$ is clearly visible.

As said above, the broadening of the observation volume worsen the autocorrelation and the time scale of $G(\tau)$ becomes progressively longer.

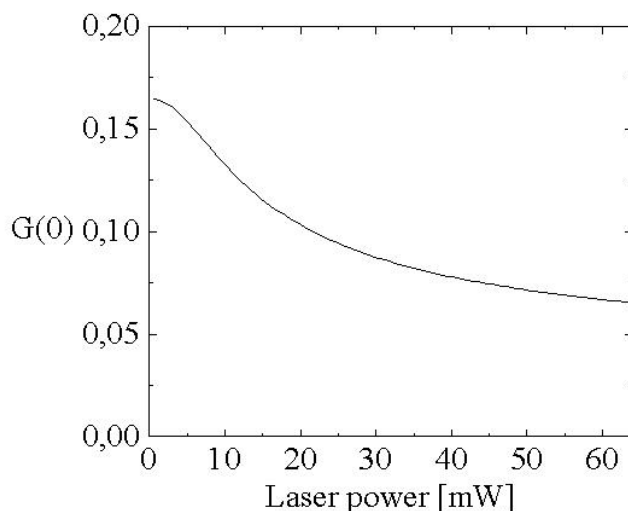


Fig. 10. Dependence of the autorrelation amplitude $G(0)$ on the laser power.

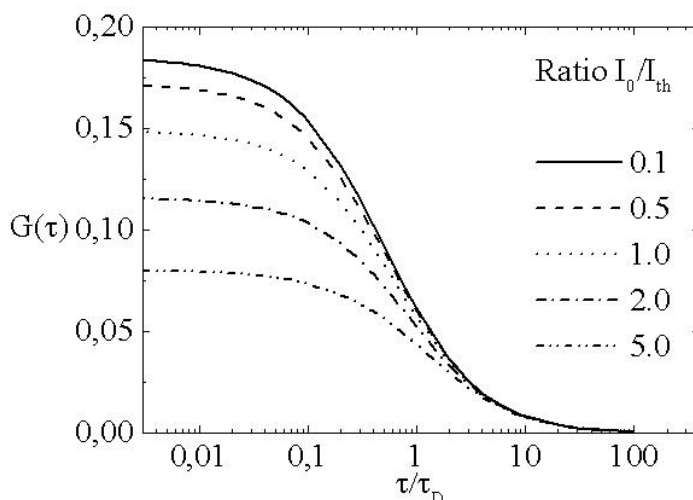


Fig. 11. Diffusional correlation function $G(\tau)$ is at different values of the ratio I_0 / I_{th}

The consequence of these results are of great impact on quantitative predictions of molecular parameters which depend on the numerical values of G as explained in Ref. [24].

Other examples of spectroscopic techniques.

Non-ideality of laser beams has so far been discussed for two spectroscopic techniques. However the applicability of the described analysis can be extended to many other spectroscopies where laser wings play an important role. For instance, Laser Induced Incandescence [25] has been proven to be sensitive to laser wings [26] and other examples might be found in literature. Among coherent spectroscopies, it might be worth citing the case of Photon-Echo Spectroscopy (PES) [1]

which has been found to suffer of self-diffraction induced by spatial laser-wings [27]. PES is used for high-resolution spectroscopy to measure population and phase decay times of atoms. The important point of PES is that inhomogeneous phase relaxation, due to Doppler-shifted frequencies of atoms at different velocities, does not eliminate the initial phase relation among the atoms, therefore the technique is Doppler-free and the homogeneous part of atomic frequency broadening can be measured. However, if the spatial non-uniformity of lasers is considered, some caution is needed in the interpretation of signals [27]. For example, signals picked in different locations of the self-diffracted far-field pattern behave in different manners and this would increase the final uncertainty contained in the experimental response.

It is possible to show that laser-wing free signals are obtainable from the detection of the whole spatial pattern of PES signals. The demonstration follows the idea already discussed for SatLIF (Eqs. (7)-(9)). The result (not shown) might be helpful because it eliminates the need of a pinhole to select spatial fragments of self-diffracted PES signal.

Conclusions

The issue of non-ideality of laser beams has been defined and examined for some spectroscopic techniques. LIF spectroscopy received a particular focus inasmuch as it represents one of the most suitable techniques applied for diagnostic purposes in fluid-dynamic environments such as flames.

The problem of spatial and temporal laser wings in SatLIF was initially addressed from a traditional point of view. However, more recent advances established by the author in this field have been reported. Unlike the traditional methods, these advances imply the detection of the whole signal emitted from the interaction region shared between the laser and the sample. The main remarkable advantage is that nothing of the signal is thrown away as opposed to the customary sampling procedures.

The new achievements have also been extended to FCS which is employed in many scientific disciplines. The role of spatial laser wings in diffusional problems has been considered and the results are confirmed by experimental data available in literature.

Other very short examples of other important spectroscopies where non-ideality of laser beams is a fundamental issue have been given.

Acknowledgements

The author thanks AIVELA for the invitation. In particular, the great support given Prof. E. P. Tomasini, Prof. N. Paone and J. Dubbini is acknowledged.

References

- [1] W. Demtröder, *Laser Spectroscopy* (Springer-Verlag, Berlin 2003).
- [2] A. C. Eckbreth, *Laser Diagnostics for Combustion Temperature and Species* (Gordon and Breach Publishers, Amsterdam 1996).
- [3] R. Riegler, *Fluorescence Correlation Spectroscopy* (Springer-Verlag, Berlin 2001).
- [4] W. P. Partridge, Jr, N. M. Laurendeau: *Appl. Opt.* **34**, 2645 (1995).
- [5] R. A. Van Calcar, M. J. M. Van de Ven, B. K. Van Uitert, K. J. Biewenga, Tj. Hollander, C. Th. J. Alkemade, *J. Quant. Spectrosc. Radiat. Transfer* **21**, 11 (1979).
- [6] C. A. Van Dijk, N. Omenetto, J. D. Winefordner, *Appl. Spectr.* **35**, 389 (1981).
- [7] There is a vast literature on SatLIF measurements. For instance: R. P. Lucht, D. W. Sweeney, N. M. Laurendeau, *Comb. Flame* **50**, 189 (1983); R. P. Lucht, D. W. Sweeney, N. M. Laurendeau, M. C. Drake, M. Lapp, R. W. Pitz, *Opt. Lett.* **9**, 90 (1984); J. T. Salmon, N. M. Laurendeau, *Appl. Opt.* **24**, 65 (1985); C. D. Carter, G. B. King, N. M. Laurendeau, *Appl. Opt.* **31**, 1511 (1992); J. R. Reisel, C. D. Carter, N. M. Laurendeau, M. C. Drake, *Combust. Sci. and Tech.* **91**, 271 (1993); C. S. Cooper, R. V. Ravikrishna, N. M. Laurendeau, *Appl. Opt.* **37**, 4823 (1998); R. V. Ravikrishna, C. S. Cooper, N. M. Laurendeau, *Comb. Flame* **117**, 810 (1999).
- [8] C. D. Carter, and N. M. Laurendeau, *Appl. Phys. B* **58**, 519 (1994).
- [9] A. B. Rodrigo, and R. M. Measures, *IEEE J. Quantum Electron.* **9**, 972 (1973).
- [10] M. Mailänder, *J. Appl. Phys.* **49**, 1256 (1978).
- [11] R. A. Van Calcar, M. J. G. Heuts, B. K. Uitert, H. A. J. Meijer, T. Hollander, and C. T. J. Alkemade, *JQSRT* **26**, 495 (1981); **28**, 1 (1982).
- [12] R. A. Van Calcar, M. J. G. Heuts, B. K. Uitert, H. A. J. Meijer, T. Hollander, and C. T. J. Alkemade, *JQSRT* **26**, 495 (1981); **28**, 1 (1982).
- [13] J. W. Daily, *Appl. Opt.* **17**, 225 (1978).
- [14] M. J. Cottreau, *Appl. Opt.* **25**, 744 (1986); P. Desgroux and M. J. Cottreau, *Appl. Opt.* **30**, 90 (1991); C. D. Carter, G. B. King, N. M. Laurendeau, *Combust. Sci. Tech.* **78**, 247 (1991).
- [15] J. T. Salmon and N. M. Laurendeau, *Appl. Opt.* **24**, 1313 (1985).
- [16] M. P. Freeman and S. Katz, *J. Opt. Soc. Am.* **53**, 1172 (1963).
- [17] M. Marrocco, *Opt. Lett.* **28**, 2016 (2003).
- [18] M. Magaldi, and M. Marrocco, *Appl. Phys. B* **76**, 699 (2003).
- [19] M. Marrocco, *Appl. Phys. B* **77**, 65 (2003).
- [20] D. Lumma, A. Best, A. Gansen, F. Feuillebois, J. O. Rädler, and O. I. Vinogradova, *Phys. Rev. E* **67**, 56313 (2003).
- [21] P. S. Dittrich, and P. Schwille, *Appl. Phys. B* **73**, 829 (2001).
- [22] R. Rigler, Ü. Metz, J. Widengren, and P. Kask, *Eur. Biophys. J* **22**, 169 (1993).
- [23] J. Widengren, and R. Rigler, *Bioimaging* **4**, 149 (1996).
- [24] K. Berland, and G. Shen, *Appl. Opt.* **42**, 5566 (2003).
- [25] See the contribution of G. Zizak in this meeting.
- [26] N. P. Tait, and D. A. Greenhalgh, *Ber. Bunsenges. Phys. Chem.* **97**, 1619 (1993).
- [27] A. I. Lvovsky, and S. R. Hartmann, *Phys. Rev. A* **59**, 4052 (1999).